Model Predictive control for Shunt Active Filters with Fixed Switching Frequency

Luca Tarisciotti, Andrea Formentini, Alberto Gaeta, Marco Degano, Pericle Zanchetta
Roberto Rabbeni, Marcello Pucci, Marco Rivera

Abstract- **This paper presents a modification to the classical Model Predictive Control algorithm, named Modulated Model Predictive Control, and its application to active power filters. The proposed control is able to retain all the advantages of a Finite Control Set Model Predictive Control whilst improving the generated waveforms harmonic spectrum. In fact a modulation algorithm, based on the cost function ratio for different output vectors, is inherently included in the MPC. The cost function-based modulator is introduced and its effectiveness on reducing the current ripple is demonstrated. The presented solution provides an effective and straightforward single loop controller, maintaining an excellent dynamic performance despite the modulated output and it is self-synchronizing with the grid. This promising method is applied to the control of a Shunt Active Filter for harmonic content reduction through a reactive power compensation methodology. Significant results obtained by experimental testing are reported and commented, showing that MPC is a viable control solution for active filtering systems.**

Keywords: **Smart Grids; Power Quality; Active Filters; Power Filters; Harmonic Distortion; Model Predictive Control.**

I. INTRODUCTION

Maintaining a good power quality level in modern electrical grids is a vital issue to ensure reliability, security and efficiency [1]. This is currently becoming extremely important due to the proliferation of non-linear loads, power conversion systems, renewable energy sources (RES), distributed generation sources (DG) and Plug-in Electric Vehicles (PEVs) [2]. Several Flexible AC Transmission System (FACTS) equipment [2], [3] have been recently investigated and applied in order to improve the electrical grid power quality. These studies resulted in a broad family of devices, such as Active and Hybrid power filters [4], [5], Static compensators (STATCOM) [6], [7], Static VAR Compensators (SVC) [8], Unified Power Flow/Quality Controllers (UPFC/UPQC) and Dynamic Voltage Restorers (DVR). In particular, Active powers filters allow to increase the overall system power quality and are not affected by the limits of their passive counterparts, such as the introduction of resonances onto the power system, impossibility of current limiting (other than fuses), overloaded operation if the supply voltage quality deteriorates [9]. However, the control of an Active Filter [10] requires fast dynamic performances and represents a challenging control problem, which may not be able to be addressed by applying linear control techniques. In fact, as a high control bandwidth is required, it may happen that the required sampling frequency became excessively high. Moreover, supply disturbances may be hard to suppress using classical PI controllers [11], [12]. Among all possible Active Filter configurations, the Shunt Active Filter (SAF) is the most

commonly applied, and several control techniques has been proposed in literature to fulfill its high bandwidth requirements. In fact, PI controllers in a stationary reference frame are unable to provide a satisfactory regulation, given the high frequency of the harmonics to control, and they fail to eliminate steady state error and to achieve satisfactory tracking of the desired reference. Other control schemes aim to improve the tracking accuracy for specified harmonics by using multiple related synchronous reference frames [13], [14]. However, the need for multiple band-pass filters and the consequent interactions among them increase the complexity of the control tuning. Alternatively, to avoid multiple reference frame transformations, Proportional Resonant (PR) controllers may be used [15]. Techniques which reduce the number of measurements required by the system have also been investigated, typically based on time domain controllers and an appropriate observer [16]. Finally, Dead-Beat control strategies have also been considered [17], coupled with a PI based DC-Link voltage control.

Model Predictive Control (MPC) has been recently adopted for power electronics converters control, due to the several benefits it can provide such as, fast tracking response and simple inclusion of system nonlinearities and constraints in the controller [18]. MPC considers the system model for predicting its future behavior and determining the best control action on the basis of a cost function minimization procedure.

Finite Control Set MPC (FCS-MPC) is a model based control strategy applicable to systems with a finite number of possible control actions, such as power electronic converters. At each sample time FCS-MPC computes a target cost function for every possible control action: the one associated to the minimum cost function value is selected as optimal control and applied [19]. This technique has been successfully applied for the control of three-phase inverters [20], [21], matrix converters [22], [23], power control in an active front end rectifiers [24], [25], and regulation of both electrical and mechanical variables in drive system applications [26]–[30].

The lack of a modulator, although being an advantage for the transient performance of the system, it is also a drawback under steady-state conditions when the high bandwidth of the control is not necessary and the higher current ripple, due to the limited set of available control actions, is more evident.

This paper presents a novel Finite Control Set Modulated MPC (FCS-M^{2}PC) algorithm suitable for SAF control, which retains most of the advantages of the MPC such as the presence of a cost function and the use of a single loop for improved responsivity and larger bandwidth, but exploits a modulator for reducing the current ripple. The cost function minimization

procedure acts also as a modulator, by selecting the best vectors and their application times for the next sampling period. A similar solution has already been proposed in [31]–[33] for a Multilevel Cascaded H-Bridge Converter, in [34], [35] for a Direct Matrix Converter and in [36] for a three phase Active Filter . Experimental results show the excellent transient and steady state performance of the proposed system.

II. SYSTEM DESCRIPTION AND MODELING

A SAF is realized by connecting a Voltage Source Converter (VSC) to the AC grid through filter inductors in a rectifier configuration. The DC side is connected to a capacitor as depicted in Fig. 1, and thus, it is able to manage only reactive power. In such configuration, the SAF is able to produce any set of balanced currents and, therefore, compensates the reactive power and current harmonics drawn by a non-linear load; clearly the SAF filtering capabilities are limited by the VSC rated power and control bandwidth. On the other hand, the grid provides only the active power required to supply the load and maintain the SAF DC-Link at the desired voltage.
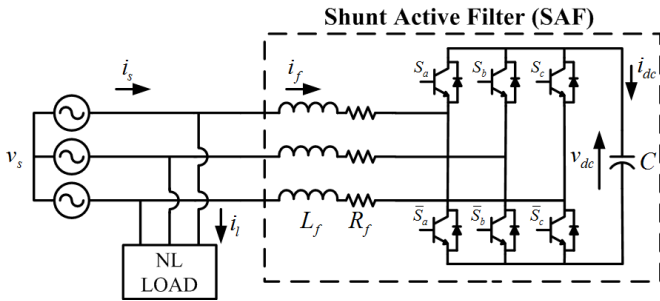
Shunt Active Filter (SAF)

Fig.1: Adopted structure of 3-wires Shunt Active Filter

When a balanced system is considered, it is possible to reduce the system order to the third order, represented in the *abc* frame by the state variables $i_{fa}(t)$, $i_{fb}(t)$ and $V_{dc}(t)$. Neglecting the nonlinearities introduced by the inverter and the equivalent impedance of the grid, the SAF currents equations can be expressed as follows:

$$\begin{cases} \frac{di_{fa}(t)}{dt} = \frac{1}{L_f} v_{sa}(t) - \frac{R_f}{L_f} i_{fa}(t) - \frac{1}{3L_f}[2S_a(t) - S_b(t) - S_c(t)]V_{dc} \\ \frac{di_{fb}(t)}{dt} = \frac{1}{L_f} v_{sb}(t) - \frac{R_f}{L_f} i_{fb}(t) - \frac{1}{3L_f}[2S_b(t) - S_a(t) - S_c(t)]V_{dc} \end{cases} \quad (1)$$

where R_f and L_f are the filter inductor winding resistance and inductance. $S_a(t)$, $S_b(t)$ and $S_c(t)$ represent each leg state, equal to 1 or 0 respectively when a positive or a negative voltage is produced at the leg output with respect to the DC-Link neutral point. The DC-Link voltage can be obtained by the converter state and the DC current, derived by the converter switching functions and AC currents, as shown in equation (2).

$$\frac{dV_{dc}(t)}{dt} = \frac{1}{C}\{[S_a(t) - S_c(t)]i_{fa}(t) + [S_b(t) - S_c(t)]i_{fb}(t)\} \quad (2)$$

Finally, the supply current can be obtained by the filter and load currents as in (3).

$$\begin{cases} i_{sa}(t) = i_{la}(t) + i_{fa}(t) \\ i_{sb}(t) = i_{lb}(t) + i_{fb}(t) \end{cases} \quad (3)$$

By combining equations (1)-(3) the SAF state space model can be derived and then discretized using Forward Euler method for control design purposes. The obtained system is shown in (4)

$$\begin{cases} i_{fa}(k+1) = \left(1 - \frac{R_f h}{L_f}\right) i_{fa}(k) - \frac{h}{L_f} Q_1 \underline{S}(k) V_{dc}(k) + \frac{h}{L_f} v_{sa}(k) \\ i_{fb}(k+1) = \left(1 - \frac{R_f h}{L_f}\right) i_{fb}(k) - \frac{h}{L_f} Q_2 \underline{S}(k) V_{dc}(k) + \frac{h}{L_f} v_{sb}(k) \quad (4) \\ V_{dc}(k+1) = V_{dc}(k) + \frac{h}{c} P_1 \underline{S}(k) i_{fa}(k) + \frac{h}{c} P_2 \underline{S}(k) i_{fb}(k) \end{cases}$$

where k represents the discrete sampling instant, h is the sampling time, and

$$Q_1 = \frac{1}{3}[2 \quad -1 \quad -1] \qquad Q_2 = \frac{1}{3}[-1 \quad 2 \quad -1]$$

$$P_1 = [1 \quad 0 \quad -1] \qquad P_2 = [0 \quad 1 \quad -1] \quad (5)$$

$$\underline{S}(k) = [S_a(k) S_b(k) S_c(k)]^T$$

III. SAF MODEL PREDICTIVE CONTROL

In FCS-MPC, due to the absence of a modulator, the only possible control actions are the ones generated by the 8 possible inverter switching states:

$$\underline{S}(k) \triangleq \left\{ \begin{bmatrix} 0 \\ 0 \\ 0 \end{bmatrix}, \begin{bmatrix} 0 \\ 0 \\ 1 \end{bmatrix}, \begin{bmatrix} 0 \\ 1 \\ 0 \end{bmatrix}, \begin{bmatrix} 0 \\ 1 \\ 1 \end{bmatrix}, \begin{bmatrix} 1 \\ 0 \\ 0 \end{bmatrix}, \begin{bmatrix} 1 \\ 0 \\ 1 \end{bmatrix}, \begin{bmatrix} 1 \\ 1 \\ 0 \end{bmatrix}, \begin{bmatrix} 1 \\ 1 \\ 1 \end{bmatrix} \right\} \quad (6)$$

At the kth time instant the controller uses equation (4) to predict the future system state value for each possible control action in (6). A cost function is then computed using a combination of predicted system states and references. The optimal control is selected by choosing the inverter configuration associated to the minimum cost function value. However, in practical implementation the computed optimal control action can be applied only at the $k+1^{th}$ time instant, due to controller computational time delay. This introduces a one-step delay in the system that must be compensated [21]. At the kth time instant, the system state at $k+1$ is predicted using the previously computed optimal control. Subsequently the procedure described before is performed starting from the $k+1^{th}$ time instant resulting in the optimal inverter switching state $S(k+1)$.

Combining the system model at the time instants $k+1$ and $k+2$, and assuming that the supply voltages can be considered constant during a sampling period h of the control algorithm (i.e. $\underline{v}_s(k) = \underline{v}_s(k+1)$) the following system is obtained.

$$\underline{X}(k+2) = A_2\left(\underline{S}(k+1)\right)\underline{X}(k) + B_2\underline{U}(k) \quad (7)$$

The definition of the matrix elements are given in Appendix I, while $\underline{X}(k)$ and $\underline{U}(k)$, shown in equation (8), represent the predicted values of active filter currents and voltages at the instant $k+2$ and the supply voltages at the time instant k.

$$\underline{X}(k+2) = \left[i_{fa}(k+2)\; i_{fb}(k+2)\; V_{dc}(k+2)\right]^T \tag{8}$$

$$\underline{U}(k) \qquad = [v_{sa}(k)\; v_{sb}(k)]^T$$

The load currents i_{la} and i_{lb} are assumed to be measurable in the considered configuration. Given the high controller sampling frequency, it is acceptable to have:

$$i_{sa}(k+2) = i_{la}(k) + i_{fa}(k+2)$$

$$i_{sb}(k+2) = i_{lb}(k) + i_{fb}(k+2) \tag{9}$$

Hence the predicted system state is defined as:

$$\underline{X}_p(k+2) = [i_{sa}(k+2)\; i_{sb}(k+2)\; V_{dc}(k+2)]^T \tag{10}$$

From (10) the control relevant variables (the active power P_s, the reactive power Q_s and the DC-Link voltage V_{dc} are predicted as shown in (11).

$$P_{sp}(k+2) = \underline{v}_s^T(k) \begin{bmatrix} 2 & 1 & 0 \\ 1 & 2 & 0 \end{bmatrix} \underline{X}_p(k+2)$$

$$Q_{sp}(k+2) = \underline{v}_s^T(k) \begin{bmatrix} 0 & \sqrt{3} & 0 \\ -\sqrt{3} & 0 & 0 \end{bmatrix} \underline{X}_p(k+2) \tag{11}$$

$$V_{dcp}(k+2) = \begin{bmatrix} 0 & 0 & 1 \end{bmatrix} \underline{X}_p(k+2)$$

The 50Hz grid voltages is supposed approximately constant in two consecutive sampling periods due to the much higher sampling frequency of the SAF control algorithm. The cost function adopted in this work to compute the optimal control action $\underline{S}(k+1)$ is defined in (12), where x^* indicate reference values and λ_1, λ_2 and λ_3 are weighting factors that allow a proper balance among deviations of the controlled variables.

$$J\left(\underline{S}(k+1)\right) = \lambda_1 \left|V_{dc}^*(k+2) - V_{dcp}(k+2)\right|$$

$$+\lambda_2 \left|P_s^*(k+2) - P_{sp}(k+2)\right| \tag{12}$$

$$+\lambda_3 \left|Q_s^*(k+2) - Q_{sp}(k+2)\right|$$

A block scheme of the complete active filter control for the case of FCS-MPC is shown in Fig. 2.

IV. MODULATED MODEL PREDICTIVE CONTROL

One of the major strength of the FCS-MPC is that it enables to include in a single control law different control targets and system constraints. In this way the traditional control of currents, voltages or flux can be combined with other requirements like common mode voltage reduction, switching frequency minimization and reactive power control. However with FCS-MPC, at each sampling time, all the possible control actions are compared by means of a cost function and only the best one is selected for the next sampling period. If the converter state is constant during a sampling period, the quantities under control are affected by a higher ripple as a consequence of the finite number of possible converter states.
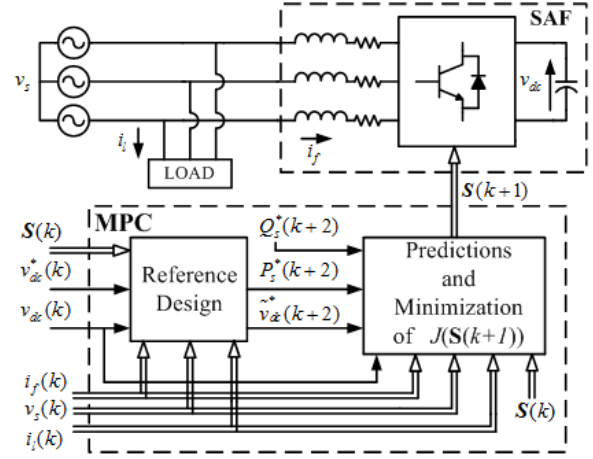

Fig.2: Schematic diagram of a FCS-MPC.

To overcome this limit, but still maintaining all the desired characteristics of FCS-MPC, this paper proposes the introduction of a suitable intrinsic modulation scheme. Consistently with the MPC approach, the cost-function is used for selecting the converter states and application times which minimize the equivalent cost in a sampling period. A symmetric PWM pattern with adjacent states has been preferred for reducing harmonics, ripple and losses. Each sampling period is composed of two zero states and two active states which are symmetrically split around the center of the sampling period. Using the predictions for the traditional FCS-MPC described in the previous section, a cost function has been defined for each sector of the $\alpha\beta$ plane as in (13), where J_i with $i = 0,1,2$ are the cost functions calculated as in (12) for the three vectors considered from the control, thus assuming $\underline{S}_i(k+1)$ equal respectively to the zero vector, the first active vector and the second active vector of the considered sector.

$$J_{sect}(k+1) = d_0 J_0 + d_1 J_1 + d_2 J_2 \tag{13}$$

Similarly d_i are the duty cycles for the zero and active vectors. They are computed assuming each duty cycle proportional to the inverse of the corresponding cost function value, where K is a normalizing constant to be determined.

$$\begin{cases} d_1 = K/J_1 \\ d_2 = K/J_2 \\ d_0 = K/J_0 \\ d_1 + d_2 + d_3 = 1 \end{cases} \tag{14}$$

Solving (14) the expression of the duty cycle is obtained as in (15).

$$d_1 = \frac{J_2}{J_1 + J_2 + \frac{J_1 J_2}{J_0}}$$

$$d_2 = \frac{J_1}{J_1 + J_2 + \frac{J_1 J_2}{J_0}} \tag{15}$$

$$d_0 = 1 - (d_1 + d_2)$$

Essentially the cost function values J_i for each sector are calculated by using (7)-(12) and the corresponding application times are calculated from (15).

The optimum sector is then determined by minimizing the cost function (13). The corresponding optimal duty cycles $\underline{d}(k+1) = [d_1(k+1)\, d_2(k+1)\, d_0(k+1)]^T$ are applied to the converter as represented in Fig.3. The switching sequence is generated from the two active and the three zero vector exactly as in a symmetrical SVM [37].
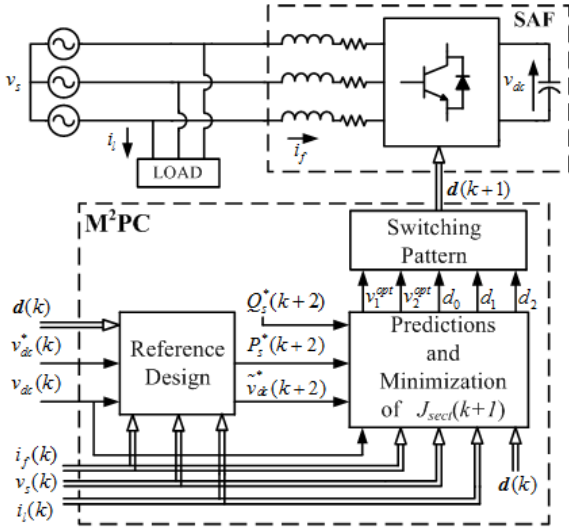

Fig.3: Schematic diagram of the proposed FCS-M2PC.

V. REFERENCES PREDICTION

The coupling between active power $P_s(k)$ and DC-Link voltage $V_{dc}(k)$, needs to be taken into account when the related reference signals are calculated. In fact, from the DC-Link voltage reference $V_{dc}^*(k)$ and the reactive power reference $Q_s^*(k)$ at the instant k, it is possible to calculate, knowing the AC current values, the active power reference at the time instant $k+2$, $P_s^*(k+2)$. Since the DC-Link capacitors compensate for the reactive power fluctuations due to the non-linear load, the dynamics of the DC-Link voltage has to be maintained considerably slower than the respective reactive power dynamic. The required change in the active power flow to regulate the voltage at the desired value is given by equation (16), where N denotes the number of time steps required for reaching the target.

$$P_{DC}(k+2) = \frac{C}{Nh}\left[V_{dc}^{*\,2}(k+2) - V_{dc}^{\,2}(k+1)\right] \quad (16)$$

The load active power reference can be calculated as in equation (17), where $\underline{i_{l1}}(k) = [i_{la1}(k)\, i_{lb1}(k)]^T$ represents the vector of the first harmonic of the load current.

$$P_l^*(k+2) = \underline{v_s^T}(k)\begin{pmatrix} 2 & 1 \\ 1 & 2 \end{pmatrix}\underline{i_{l1}}(k) \quad (17)$$

Thanks to the high controller sampling frequency, it is acceptable to approximate $\underline{i_{l1}}(k) = \underline{i_{l1}}(k+2)$. The active power $P_l^*(k+2)$ is simply obtained by filtering (17) with a digital resonant filter having a resonance frequency equal to 50Hz. Finally, the total reference power at the supply side is therefore:

$$P_s^*(k+2) = P_l^*(k+2) + P_{DC}(k+2) \quad (18)$$

Equation (18), together with $Q_s^*(k+2) = 0$ (to ensure unity power factor operation of the system) and $V_{dc}^*(k+2)$ constitute the reference set for the cost function (12). The minimization of active and reactive power errors allows also an automatic and fast synchronization with the grid as demonstrated by the presented results in Section VI and VII.

VI. SIMULATION RESULTS

Simulation tests have been performed to validate the proposed control system and investigate its stability. The control target is to maintain the SAF DC-Link regulated at the reference value of *700V* while filtering the nonlinear load harmonics through an inductive filter, whose rated parameters are L_f=4.75mH, R_f=0.4Ω.

Fig. 4 shows the M²PC effectiveness at rated conditions (Fig. 4b) and the proposed control response to filter inductance variations around the nominal value. When L_f is equal to the nominal value, the one taken into account in the control design, the best control response is obtained with minimal supply current distortions. On the other hand when the filter inductance varies the control performance starts degrading, but still maintaining a stable and acceptable behaviour for large mismatch of L_f hence ensuring a good control robustness. In particular when the filter inductance value is lower than the nominal value higher frequency distortions, related with the degraded modulation performance, are present. Vice-versa, when the filter inductance value is higher than the nominal value, lower frequency distortions, related with a control tracking delay, are present. In any case the M²PC control is able to maintain stable operation with slightly downgraded performance for filter inductance variations from 50% to 200% the nominal value, as shown in Table I.

TABLE I CONTROL SENSITIVITY TO PARAMETERS VARIATION

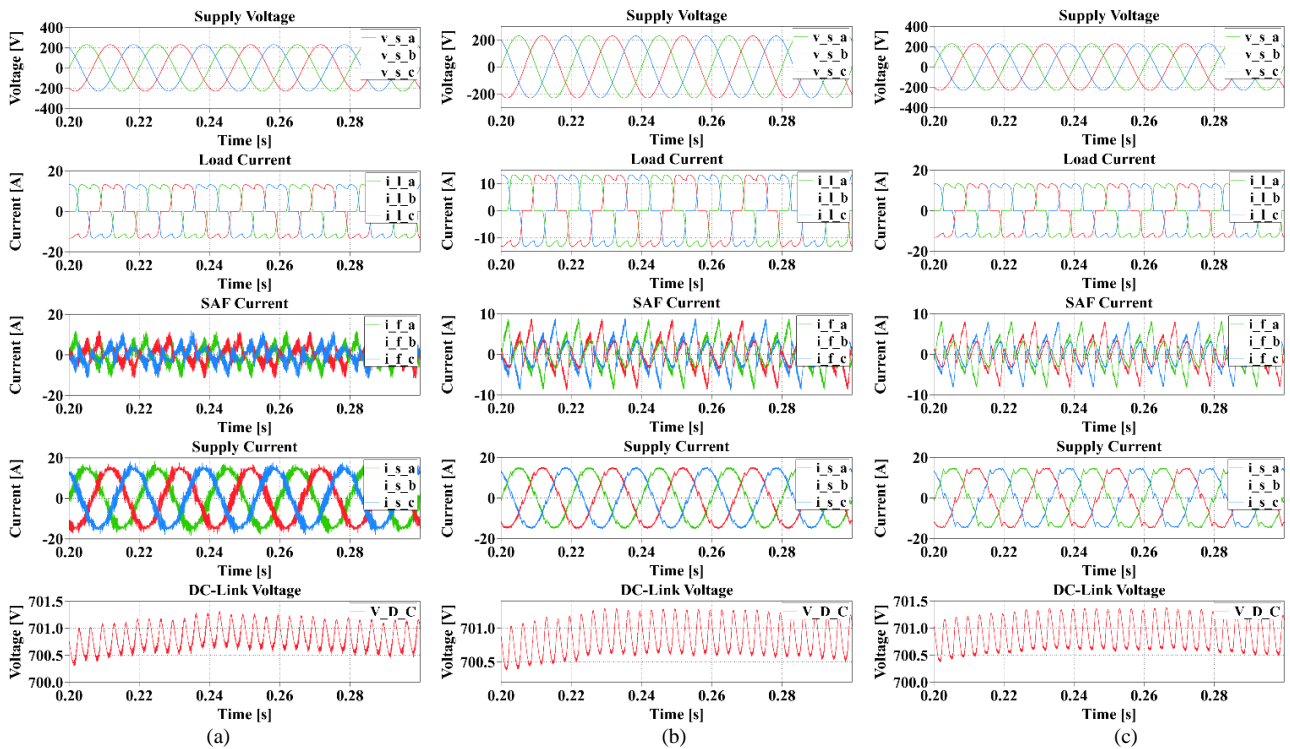|	L_F VALUE CONSIDERED IN THE SYSTEM	SUPPLY CURRENT THD
50% L_F	2.375 mH	14.7159 %
75% L_F	3.5625 mH	5.70214 %
L_F	4.75 mH	5.56090 %
125% L_F	5.90 mH	6.38301 %
150% L_F	7.10 mH	7.51365 %
200% L_F	9,50 mH	9.72609 %

Fig.4: M2PC sensitivity to filter inductance variation: (a) Lf = 2.375mH (b) Lf = 4.75mH (c) Lf = 9.5mH.

VII. EXPERIMENTAL RESULTS

A prototype SAF, with the scheme of Fig. 1, has been used to experimentally investigate the actual performances of the proposed control strategy. The SAF experimental prototype includes a classical two level Voltage Source Converter based on IGBT devices, rated *15 A*, with a DC-Link nominal voltage of *700 V*. The DC-Link is composed of a capacitors bank with *2200μF* capacity. The AC is connected to the mains Point of Common Coupling (PCC) using a three phase inductive filter whose equivalent series parameters are L_f=*4.75mH*, R_f=*0.4Ω*. The control system is composed of a TMS320C6713®Digital Signal Processor (DSP) clocked at 225 MHz and of an auxiliary board equipped with a ProASIC3 A3P400® Field Programmable Gate Array (FPGA) clocked at 50 MHz. The DSP and FPGA boards may be noticed on top of the prototype SAF of Fig. 5, shown without the AC side inductors.
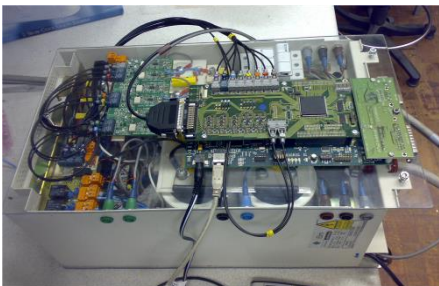

Fig.5: Top view of the experimental SAF prototype.

A three phase diode bridge rectifier has been used as nonlinear load in order to create a distorted grid current. The diode rectifier supplies a resistor with rated power P_l=*5kW*. A standard three phase 230Vrms 50Hz grid has been used for the experimental test.

In order to validate the effectiveness of the proposed solution, the FCS-M²PC has been tested and compared against the standard FCS-MPC. A fixed sampling frequency of 50kHz and 20kHz have been used for the FCS-MPC for the FCS-M²PC respectively. A steady-state test under full load P_l=5kW and a transient test for a 50% to 100% load variation are shown in Fig. 6 and Fig 7 for the FCS-MPC.

As it can be appreciated from Fig. 6, the current harmonic distortion caused by the presence of the nonlinear load, shown in Fig. 6a where the vertical axis measures 5A/div while the horizontal one 10ms/div, are actively compensated from the filtering system. The main current does not presents particular harmonic distortions (5A/div), as shown in Fig. 6b, and are in phase with the main voltage (100V/div) as desired. The SAF allows quasi-sinusoidal current and unity power factor operation. However the mains current shows an high-frequency ripple related with the variable switching frequency and the absence a Pulse Width Modulation technique, typical of FCS-MPC control. Fig 6c shows the harmonic filtering by comparing the spectrum of the mains compensated currents with the one of the nonlinear load currents. The results show a reduction of THD from THD>29% to *THD<7%*, where the THD is calculated including up to the 40th harmonic. A load current variation, realized by stepping up the rectifier load from 50% to 100%, is represented in Fig. 7a while the waveforms of mains voltage and current for one of the phases during such transient are reported in Fig. 7b, presenting the same axis measures as Fig. 6a and Fig. 6b.
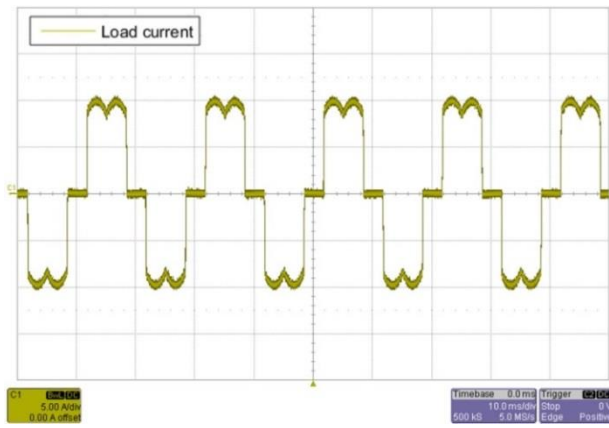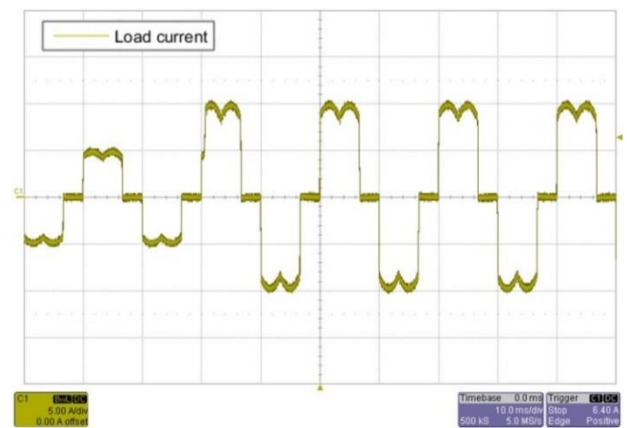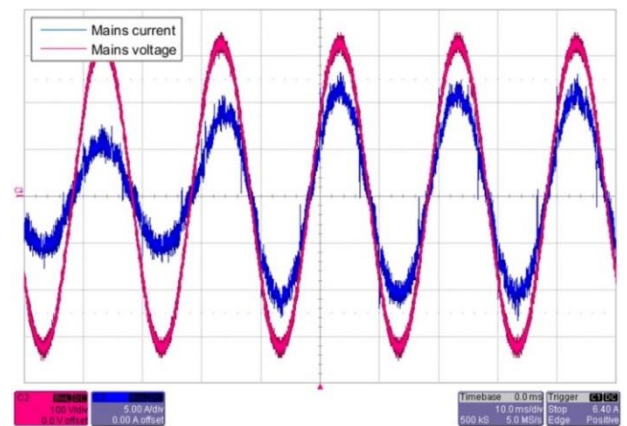
(a)
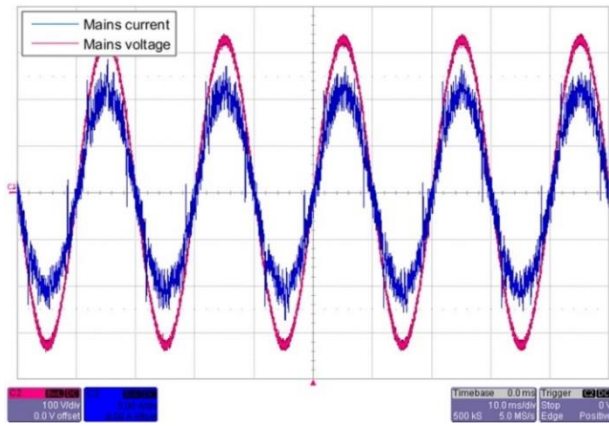
(b)
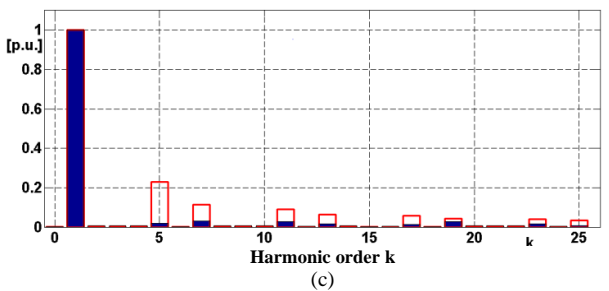
(c)

Fig.6: Steady state performance for FCS-MPC under full load [10 ms/div]: (a) current in the non-linear load [5A/div]; (b) mains current [5A/div] and mains voltage [100V/div]; (c) Spectrum of currents in (a) and (b).

(a)

(b)

(c)

Fig.7: Transient performance for FCS-MPC during a 50% to 100% load variation [10 ms/div]: (a) current in the non-linear load [5A/div]; (b) mains current [5A/div] and mains voltage [100V/div]; (c) dc-link voltage [5V/div].

It can be noticed that the SAF takes about half fundamental period to reach steady state conditions after the transient, exhibiting a very fast dynamics and accurate tracking performances. Fig. 7c shows the DC-Link voltage which remains well-regulated with a maximum ripple equal to 0.7% of its nominal value.
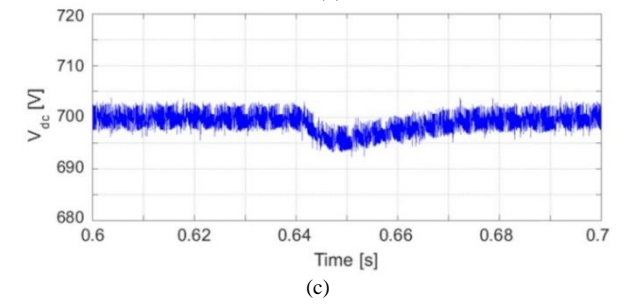
Similar tests were performed for the FCS-M^{2}PC and are shown in Fig.8 and Fig.9. As it can be noticed, the high frequency ripple in the mains current is considerably reduced by the modulation. The dynamic performances of the FCS-M^{2}PC during the sudden load changes are qualitatively similar to the standard MPC ones. Compared with FCS-MPC, the proposed control technique presents a similar harmonic content (up to the 40th harmonic) for the mains current, as

shown in Fig. 8b. However, it should be considered that the sampling frequencies are different for the two controllers, respectively 20KHz for the FCS-M^{2}PC and 50KHz for the MPC. In fact MPC requires a higher sampling frequency compared to fixed switching frequency modulated approaches (given the resulting much lower average switching frequency) and this may result in extreme specification for the control system design, in term of computational speed, thus increasing its cost. Nevertheless when FCS-M^{2}PC is utilized, the mains current THD is reduced from 29% to less than 6% by the SAF, performing well even at lower sampling frequencies. Moreover, by increasing the FCS-M^{2}PC sampling frequency a further mains current THD reduction is achievable.
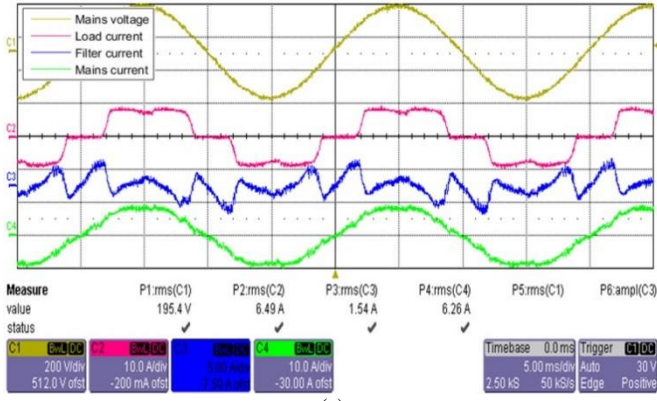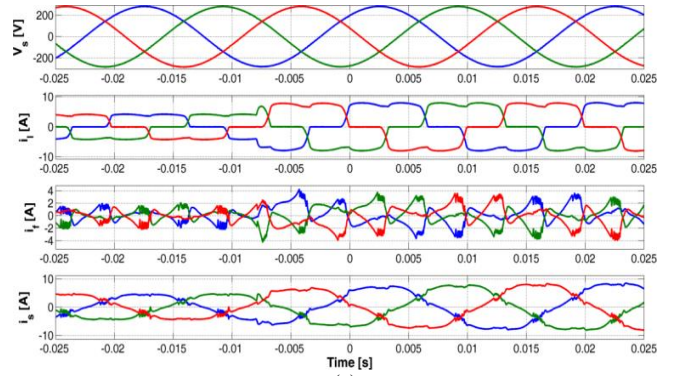
(a)
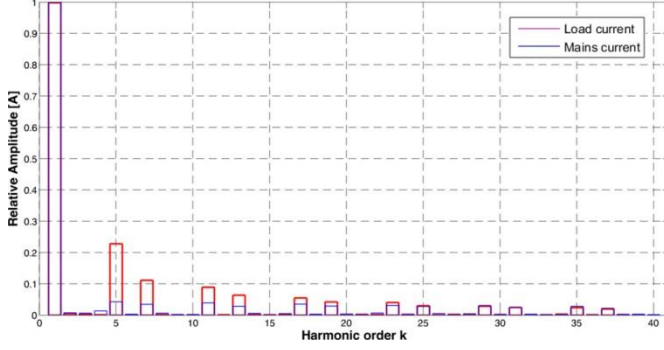
(b)

Fig.8: Steady state performance for FCS-M²PC under full load [5 ms/div]: (a) mains voltage [200V/div], load current [10A/div], filter current [2A/div] and mains current [10A/div]; (b) Spectrum of load current (red) and mains current (blue) in (a).

(a)

(b)

Fig.9: Transient performance for FCS-M²PC during a 50% to 100% load variation: (a) mains voltages [200V/div], load currents [10A/div], filter currents [2A/div] and mains currents [10A/div], [5 ms/div]; (b) reference and measured dc-link voltages [2V/div], [50ms/div].

The performance during the load change remains good and, in overall terms, the power quality improvement achieved by means of the examined SAF results excellent. This confirms the validity of the proposed solution and the viability of FCS-M²PC for SAF control and grid synchronization, employing a single compact control loop that regulates all system relevant quantities.
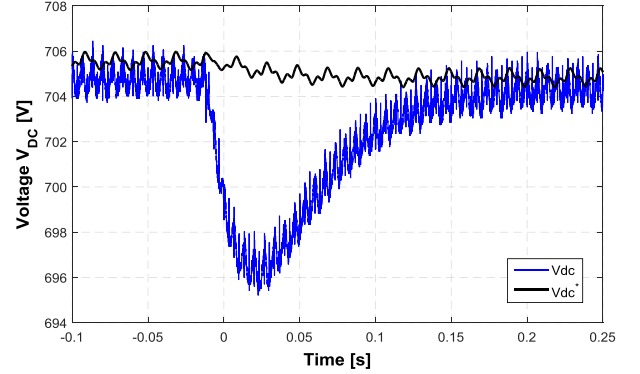
VIII. CONCLUSIONS

Power quality regulation is a relevant topic in modern electrical networks. Improving the quality of the delivered energy is an important characteristic in the new smart grids where there is an increasing demand of dynamic, efficient and reliable distribution systems. The use of active filters becomes therefore vital for the reduction of harmonic distortions in the power grid. This paper has presented the development and the implementation of a SAF for harmonic distortion reduction regulated by an improved Modulated Model Predictive Controller.

Based on the system model, it dynamically predicts the values of all the variable of interest in order to obtain a multiple control target optimization by minimizing a user defined cost function. Moreover the higher current ripple typical of MPC has been considerably reduced by introducing a cost function-based modulation strategy without compromising the dynamic performances. A SAF prototype implementing the proposed

solution was then described, finally reporting and commenting the promising experimental tests results both in transient conditions and steady-state. It was hence demonstrated that FCS-M²PC is a viable and effective solution for control of active power compensators, where different systems variables can be regulated with the aid of only a single control loop, with no need for grid synchronization devices.

APPENDIX I

DEFINITION OF MATRIX ELEMENTS IN (7)

$$A_2 = \begin{bmatrix} a11 & a12 & a13 \\ a21 & a22 & a23 \\ a31 & a32 & a33 \end{bmatrix} B_2 = \begin{bmatrix} b11 & 0 \\ 0 & b22 \\ b31 & b32 \end{bmatrix}$$

$$a11 = \left(1 - \frac{R_f h}{L_f}\right)^2 - \frac{h^2}{L_f C} Q_1 \underline{S}(k+1) P_1 \underline{S}(k)$$

$$a12 = -\frac{h^2}{L_f C} Q_1 \underline{S}(k+1) P_2 \underline{S}(k)$$

$$a13 = -\frac{h}{L_f} Q_1 \left[\left(1 - \frac{R_f h}{L_f}\right) \underline{S}(k) + \underline{S}(k+1)\right]$$

$$a21 = -\frac{h^2}{L_f C} Q_2 \underline{S}(k+1) P_1 \underline{S}(k)$$

$$a22 = \left(1 - \frac{R_f h}{L_f}\right)^2 - \frac{h^2}{L_f C} Q_2 \underline{S}(k+1) P_2 \underline{S}(k)$$

$$a23 = -\frac{h}{L_f}Q_2\left[\left(1-\frac{R_f h}{L_f}\right)\underline{S}(k)+\underline{S}(k+1)\right]$$

$$a31 = \frac{h}{C}P_1\left[\underline{S}(k)+\left(1-\frac{R_f h}{L_f}\right)\underline{S}(k+1)\right]$$

$$a32 = \frac{h}{C}P_2\left[\underline{S}(k)+\left(1-\frac{R_f h}{L_f}\right)\underline{S}(k+1)\right]$$

$$a33 = 1-\frac{h^2}{L_f C}\left[P_1\underline{S}(k+1)Q_1\underline{S}(k)+P_2\underline{S}(k+1)Q_2\underline{S}(k)\right]$$

$$b11 = b22 = \frac{h(2L_f-R_f h)}{L_f^2} \quad b31 = \frac{h^2}{L_f C}P_1\underline{S}(k+1) \quad b32 = \frac{h^2}{L_f C}P_2\underline{S}(k+1)$$

REFERENCES

[1] P. Salmeron and S. P. Litran, "Improvement of the Electric Power Quality Using Series Active and Shunt Passive Filters," *IEEE Trans. Power Del.*, vol. 25, no. 2, pp. 1058–1067, 2010.

[2] H. Johal and D. Divan, "Design Considerations for Series-Connected Distributed FACTS Converters," *IEEE Trans. Ind. Appl.*, vol. 43, no. 6, pp. 1609–1618, 2007.

[3] D. Divan and H. Johal, "Distributed FACTS—A New Concept for Realizing Grid Power Flow Control," *IEEE Trans. Power Electron.*, vol. 22, no. 6, p. 2253, 2007.

[4] B. Singh, K. Al-Haddad, and A. Chandra, "A review of active filters for power quality improvement," *IEEE Trans. Ind. Electron.*, vol. 46, no. 5, pp. 960–971, 1999.

[5] M. L. Heldwein, H. Ertl, J. Biela, D. Das, R. P. Kandula, J. A. Munoz, D. Divan, R. G. Harley, and J. E. Schatz, "An Integrated Controllable Network Transformer—Hybrid Active Filter System," *IEEE Trans. Ind. Appl.*, vol. 51, no. 2, pp. 1692–1701, 2015.

[6] S. W. Mohod and M. V. Aware, "A STATCOM-Control Scheme for Grid Connected Wind Energy System for Power Quality Improvement," *IEEE Syst. J.*, vol. 4, no. 3, pp. 346–352, 2010.

[7] S. Wenchao and A. Q. Huang, "Fault-Tolerant Design and Control Strategy for Cascaded H-Bridge Multilevel Converter-Based STATCOM," *IEEE Trans. Ind. Electron.*, vol. 57, no. 8, pp. 2700–2708, 2010.

[8] A. Hamadi, S. Rahmani, and K. Al-Haddad, "A Hybrid Passive Filter Configuration for VAR Control and Harmonic Compensation," *IEEE Trans. Ind. Electron.*, vol. 57, no. 7, pp. 2419–2434, 2010.

[9] R. C. Dugan, M. F. McGranaghan, and H. W. Beaty, *Electrical power systems quality*. McGraw-Hill, 1996.

[10] H. Akagi, "The state-of-the-Art of Active Filters for Power Conditioning," *Eur. Conf. Power Electron. Appl.*, p. 15, 2005.

[11] S. Buso, L. Malesani, and P. Mattavelli, "Comparison of Current Control Techniques for Active Filter Applications," *IEEE Trans. Ind. Electron.*, vol. 45, no. 5, pp. 722–729, 1998.

[12] P. Jintakosonwit, H. Fujita, and H. Akagi, "Control and performance of a fully-digital-controlled shunt active filter for installation on a power distribution system," *IEEE Trans. Power Electron.*, vol. 17, no. 1, pp. 132–140, 2002.

[13] D. N. Zmood, D. G. Holmes, and G. H. Bode, "Frequency-domain analysis of three-phase linear current regulators," *IEEE Trans. Ind. Appl.*, vol. 37, no. 2, pp. 601–610, 2001.

[14] E. H. J.M., C.-M. J., F. J.R., and G.-G. R., "A synchronous Reference Frame Robust Predictive Current Control for Three-Phase Grid-Connected Inverters," *IEEE Trans. Ind. Electron.*, vol. 57, no. 3, pp. 954–962, 2010.

[15] P. Mattavelli, "A Closed Loop Selective Harmonic Compensation for Active Filters," *IEEE Trans. Ind. Appl.*, vol. 37, no. 1, pp. 81–89, 2001.

[16] K. H. Kwan, P. L. So, and Y. C. Chu, "A harmonic selective unified power quality conditioner using MVR with Kalman filters," *Int. Power Eng. Conf.*, pp. 332–337, 2007.

[17] L. Malesani, P. Mattavelli, and S. Buso, "Robust dead-beat current control for PWM rectifiers and active filters," *IEEE Trans. Ind. Appl.*, vol. 35, no. 3, pp. 613–620, 1998.

[18] S. Kouro, P. Cortés, R. Vargas, U. Ammann, and J. Rodríguez, "Model predictive control—A simple and powerful method to control power converters," *IEEE Trans. Ind. Electron.*, vol. 56, no. 6, pp. 1826–1838, 2009.

[19] J. Rodríguez and M. P. Kazmierkowski, "State of the Art of Finite Control Set Model Predictive Control in Power Electronics," *IEEE Trans. Ind. Informat.*, vol. 9, no. 2, pp. 1003–1016, 2013.

[20] R. P. Aguilera, P. Lezana, and D. E. Quevedo, "Finite-Control-Set Model Predictive Control With Improved Steady-State Performance," *IEEE Trans. Ind. Informat.*, vol. 9, no. 2, pp. 658–667, May 2013.

[21] L. Tarisciotti, P. Zanchetta, A. Watson, J. C. Clare, S. Member, M. Degano, and S. Bifaretti, "Modulated Model Predictive Control for a Three-Phase Active Rectifier," *IEEE Trans. Ind. Appl.*, vol. 51, no. 2, pp. 1610–1620, 2015.

[22] M. Rivera, C. Rojas, J. Rodríguez, P. Wheeler, B. Wu, and J. R. Espinoza, "Predictive Current Control With Input Filter Resonance Mitigation for a Direct Matrix Converter," *IEEE Trans. Power Electron.*, vol. 26, no. 10, pp. 2794–2803, 2011.

[23] M. Rivera, L. Tarisciotti, P. Zanchetta, and P. Wheeler, "Predictive control of an indirect matrix converter operating at fixed switching frequency and without weighting factors," *IEEE Int. Symp. Ind. Electron.*, pp. 2163–5145, 2015.

[24] Z. Zhang, H. Fang, and R. Kennel, "Fully FPGA based direct model predictive power control for grid-tied AFEs with improved performance," *41st Annu. Conf. IEEE Ind. Electron. Soc.*, pp. 3881–3886, 2015.

[25] B. Arif, L. Tarisciotti, P. Zanchetta, J. C. Clare, and M. Degano, "Grid Parameter Estimation Using Model Predictive Direct Power Control," *IEEE Trans. Ind. Appl.*, vol. 51, no. 6, pp. 4614–4622, 2015.

[26] L. Rovere, A. Formentini, A. Gaeta, P. Zanchetta, and M. Marchesoni, "Sensorless Finite Control Set Model Predictive Control for IPMSM Drives," *IEEE Trans. Ind. Electron.*, vol. 63, no. 9, pp. 5921–5931, 2016.

[27] A. Formentini, L. de Lillo, M. Marchesoni, A. Trentin, P. Wheeler, and P. Zanchetta, "A new mains voltage observer for PMSM drives fed by matrix converters," in *EPE*, 2014, pp. 1–10.

[28] E. Fuentes, D. Kalise, J. Rodríguez, and R. M. Kennel, "Cascade-Free Predictive Speed Control for Electrical Drives," *IEEE Trans. Ind. Electron.*, vol. 61, no. 5, pp. 2176–2184, 2014.

[29] M. Preindl and S. Bolognani, "Model Predictive Direct Speed Control with Finite Control Set of PMSM Drive Systems," *IEEE Trans. Power Electron.*, vol. 28, no. 2, pp. 1007–1015, 2013.

[30] A. Formentini, A. Trentin, M. Marchesoni, P. Zanchetta, and P. Wheeler, "Speed Finite Control Set Model Predictive Control of a PMSM Fed by Matrix Converter," *IEEE Trans. Ind. Electron.*, vol. 62, no. 11, pp. 6786–6796, 2015.

[31] L. Tarisciotti, P. Zanchetta, A. Watson, P. Wheeler, J. C. Clare, and S. Bifaretti, "Multiobjective Modulated Model Predictive Control for a Multilevel Solid-State Transformer," *IEEE Trans. Ind. Appl.*, vol. 51, no. 5, pp. 4051–4060, 2015.

[32] L. Tarisciotti, P. Zanchetta, A. J. Watson, J. C. Clare, S. Bifaretti, and M. Rivera, "A new Predictive Control method for cascaded multilevel converters with intrinsic modulation scheme," *IEEE Annu. Conf. Ind. Electron.*, pp. 5764–5769, 2013.

[33] L. Tarisciotti, P. Zanchetta, A. Watson, J. Clare, and S. Bifaretti, "Modulated Model Predictive Control for a 7-Level Cascaded H-Bridge back-to-back Converter," *IEEE Trans. Ind. Electron.*, vol. 61, no. 10, pp. 5375–5383, 2014.

[34] M. Vijayagopal, L. Empringham, L. De Lillo, L. Tarisciotti, P. Zanchetta, and P. Wheeler, "Current control and reactive power minimization of a direct matrix converter induction motor drive with Modulated Model Predictive Control," *IEEE Int. Symp. Predict. Control Electr. Drives Power Electron.*, pp. 4315–4321, 2015.

[35] M. Vijayagopal, L. Empringham, L. De Lillo, L. Tarisciotti, P. Zanchetta, and P. Wheeler, "Control of a Direct Matrix Converter Induction Motor Drive with Modulated Model Predictive Control," *IEEE Energy Convers. Congr. Expo.*, pp. 4315–4321, 2015.

[36] R. Rabbeni, L. Tarisciotti, A. Gaeta, A. Formentini, P. Zanchetta, M. Pucci, M. Degano, and M. Rivera, "Finite states modulated model predictive control for active power filtering systems," *IEEE Energy Convers. Congr. Expo.*, pp. 1556–1562, 2015.

[37] L. Tarisciotti, P. Zanchetta, A. J. Watson, J. C. Clare, M. Degano, and S. Bifaretti, "Modulated Model Predictve Control (M2PC) for a 3-Phase Active Front-End," in *IEEE Energy Conversion Congress and Exposition (ECCE)*, 2013, pp. 1062–1069.

Luca Tarisciotti (S'12-M'15) received the Master's degree in electronic engineering from The University of Rome "Tor Vergata" in 2009 and his Ph.D. degree in Electrical and Electronic Engineering from the PEMC group, University of Nottingham in 2015. He is currently working as Research Fellow at the University of Nottingham, UK. His research interests includes matrix converters, DC/DC converters, multilevel converters, advanced modulation schemes, and advanced power converter control.

Andrea Formentini was born in Genova, Italy, in 1985. He received the M.S. degree in computer engineering and the PhD degree in electrical engineering from the University of Genova, Genova, in 2010 and 2014 respectively. He is currently working as research fellow in the Power Electronics, Machines and Control Group, University of Nottingham. His research interests include control systems applied to electrical machine drives and power converters.

Alberto Gaeta (S' 08) received the M.S. and Ph.D degrees in electrical engineering from the University of Catania, Catania, Italy, in 2008 and 2011, respectively. From 2013 to 2015 he joined the Power Electronics and Machine Control Group at the University of Nottingham. Currently he works as a consultant for several comnpanies. He is a member of the IEEE Industrial Electronics, IEEE Industry Applications, IEEE Power Electronics Societies. His research interests include power electronics and high performance drives, with particular attention to predictive, fault tolerant and sensorless control techniques.

Marco Degano (S'03–M'07) received the 5 years Laurea Degree in Electronic Engineering from the Universita' degli studi di Udine (Italy) in April 2004. Since February 2008 he joined the Power Electronics Machines and Control (PEMC) research group at the University of Nottingham starting first as a visiting research fellow within the Marie Curie program, then in October 2012 he received his PhD degree in Electrical and Electronic Engineering; he is currently a research fellow. His current research interests are in the field of power electronic, especially for aerospace.

Pericle Zanchetta (M'00–SM'15) received his Master degree in Electronic Engineering and his Ph.D. in Electrical Engineering from the Technical University of Bari (Italy) in 1994 and 1998 respectively. In 1998 he became Assistant Professor of Power Electronics at the same University. In 2001 he became lecturer in control of power electronics systems in the PEMC research group at the University of Nottingham – UK, where he is now Professor in Control of Power Electronics systems. He has published over 220 peer reviewed papers; he is Chair of the IAS Industrial Power Converter Committee (IPCC) and associate editor for the IEEE transactions on Industry applications and IEEE Transaction on industrial informatics. He is member of the European Power Electronics (EPE) Executive Council. His general research interests are in the field of Power Electronics, Power Quality, Renewable energy systems and Control.

Marcello Pucci (M'03–SM'11) received his "laurea" degree in Electrical Engineering from the University of Palermo (Italy) in 1997 and the Ph.D. degree in Electrical Engineering in 2002 from the same University. In 2000 he has been an host student at the Institut of Automatic Control of the Technical University of Braunschweig, Germany, working in the field of control of AC machines, with a grant from DAAD (Deutscher Akademischer Austauscdienst – German Academic Exchange Service). From 2001 to 2007 he has been a researcher and since 2008 he has been a senior researcher at the Section of Palermo of I.S.S.I.A.-C.N.R. (Institute on Intelligent Systems for the Automation), Italy. He serves as an associate editor of the IEEE Transactions on Industrial Electronics and IEEE Transactions on Industry Applications. He is a member of the Editorial Board of the "Journal of Electrical Systems". His current research interests are electrical machines, control, diagnosis and identification techniques of electrical drives, intelligent control and power converters. He is a senior member of the IEEE.

Roberto Rabbeni was born in Petralia Sottana, Italy, in 1987. He received the Master's degree in automation engineering from the University of Palermo, Palermo, Italy, in 2013, where he is currently working toward the Ph.D. degree in system and control engineering in the Department of Energy, Information Engineering and Mathematical Model. His research interests focus on the development of feedback control algorithms for nonlinear dynamical systems, identification techniques, and estimation of dynamical systems. He is also interested in applications of control of power converters, electrical drives, and mechanical systems.

Marco Rivera (S'09–M'11) received his B.Sc.in Electronics Engineering and M.Sc. in Electrical Engineering from the Universidad de Concepcion, Chile in 2007 and 2008, respectively. He recieved his Ph.D. degree at the Department of Electronics Engineering, Universidad Tecnica Federico Santa Maria (UTFSM), in Valparaiso, Chile, in 2011. He is currently Associate Professor in the Department of Industrial Technologies at Universidad de Talca, Curico, Chile. His main research areas are digital control applied to power electronics, matrix converters, predictive control and control of power converters for renewable energy applications.